

Connecting Border Collision With Saddle-Node Bifurcation in Switched Dynamical Systems

Yue Ma, Chi K. Tse, *Senior Member, IEEE*, Takuji Kousaka, *Member, IEEE*, and Hiroshi Kawakami, *Member, IEEE*

Abstract—Switched dynamical systems are known to exhibit border collision, in which a particular operation is terminated and a new operation is assumed as one or more parameters are varied. In this brief, we report a subtle relation between border collision and saddle-node bifurcation in such systems. Our main finding is that the border collision and the saddle-node bifurcation are actually linked together by unstable solutions which have been generated from the same saddle-node bifurcation. Since unstable solutions are not observable directly, such a subtle connection has not been known. This also explains why border collision manifests itself as a “jump” from an original stable operation to a new stable operation. Furthermore, as the saddle-node bifurcation and the border collision merge tangentially, the connection shortens and eventually vanishes, resulting in an apparently continuous transition at border collision in lieu of a “jump.” In this brief, we describe an effective method to track solutions regardless of their stability, allowing the subtle phenomenon to be uncovered.

Index Terms—Border collision, saddle-node bifurcation, switched dynamical systems, unstable solutions.

I. INTRODUCTION

BEING a commonly observed phenomenon in switched dynamical systems, border collision has attracted much attention in recent years [1]–[4]. Like other typical bifurcation scenarios, border collision manifests itself as a sudden change of qualitative behavior of a system as one or more parameters are varied and hence can be regarded as a kind of *bifurcation* phenomenon. However, border collision has always been considered separately from such traditional bifurcations as saddle-node bifurcation and period-doubling bifurcation. This can be attributed to the fundamental difference in the mechanisms underlying border collision and traditional bifurcations. Specifically, traditional bifurcations are caused by a loss of stability of an operating orbit and the assumption of a new stable orbit, whereas border collision is resulted from operational change in which an operating orbit fails to maintain itself due to some inherent structural property of the system [5]. The system thus typically jumps to another stable operating orbit at border collision. Moreover, no loss of stability is required

Manuscript received August 22, 2004. This work was supported by the Hong Kong Research Grant Council under a CERG Grant PolyU 5241/03E. This paper was recommended by Associate Editor M. di Bernardo.

Y. Ma and H. Kawakami are with the Electrical and Electronic Engineering Department, The University of Tokushima, 770-8506 Tokushima, Japan (e-mail: mayue@ee.tokushima-u.ac.jp).

C. K. Tse is with the Department of Electronic and Information Engineering, Hong Kong Polytechnic University, Hong Kong (e-mail: encktse@polyu.edu.hk).

T. Kousaka is with the Department of Electronic and Electrical Engineering, Fukuyama University, 729-0292, Fukuyama City, Japan (e-mail: kousaka@fuee.fukuyama-u.ac.jp).

Digital Object Identifier 10.1109/TCSII.2005.850488

for border collision. Up to now, because of the apparent lack of commonality between border collision and traditional bifurcations, no connection has been known that links the two types of coexisting bifurcations in a given switched dynamical system.

In our previous work [6], the relation between border collision and period-doubling bifurcation has been discussed briefly. In this brief, we will find a strong link that connects border collision with saddle-node bifurcation. Specifically, by tracking the border collision that occurs in unstable periodic solutions, we will show how border collision is connected to a coexisting saddle-node bifurcation via unstable solutions. Based on this finding, we are able to explain why and when a “jump” or “continuous transition” occurs during border collision.

II. SADDLE-NODE BIFURCATION AND BORDER COLLISION

Suppose that $x_0 \in R^n$ is a fixed point of the map T , i.e.,

$$x_0 - T(x_0) = 0. \quad (1)$$

The characteristic equation can be written as

$$\begin{aligned} \chi(\mu) &= \det[\mu I_n - DT(x_0)] \\ &= \mu^n + a_1 \mu^{n-1} + \cdots + a_{n-1} \mu + a_n = 0. \end{aligned} \quad (2)$$

Typically, the coefficients of this characteristic equation are parameter-dependent and can be varied by varying one or more parameters. At a bifurcation point, hyperbolicity is violated and the characteristic multipliers reach a critical distribution [7]. For saddle-node bifurcation, one of the characteristic multipliers satisfies the condition $\mu = 1$. Such a bifurcation can produce or destroy a pair of solutions: one is a node (${}_0O$) and the other is a one-dimensional (1-D) unstable saddle (${}_1O$).

A border collision is a bifurcation phenomenon which is often observed in switched dynamical systems. Unlike traditional bifurcations, border collision is independent of the movement of the characteristic multipliers as parameters are varied. Instead, it occurs when the system experiences a structural change which causes a stable operation to cease, as a result of the system state hitting a spatial or temporal “border” [5], [6]. Specifically, in our previous work [6], a method has been proposed to locate the occurrence of border collision. However, the manifestation of the transition at border collision (i.e., the way in which the system jumps from one orbit to another) is still a complicated problem which is not generally solved.

In much of the previous study, only stable solutions are considered in detail, as limited by the way in which codimension-1 bifurcation diagrams are obtained through deriving the steady-state solutions of the system. In the following, we will introduce

a method to compute the fixed points of switched dynamical systems regardless of their stability. Then, by tracking the bifurcation of unstable solutions, we are able to uncover an important role that unstable solutions play in connecting border collision and saddle-node bifurcation.

III. PERIODIC SOLUTIONS AND STABILITY

A switched dynamical system can be described briefly as follows. Consider a simple but general case where a switched dynamical system consists of two subsystems: $S_1 : \dot{x} = f(x, \lambda_1)$, $x \in R^n$ and $S_2 : \dot{x} = g(x, \lambda_2)$, $x \in R^n$, where x and λ denote the state variables and system parameters, respectively. Solution flows of the subsystems are represented by $\varphi(t, x_{f0})$ and $\psi(t, x_{g0})$, where x_{f0} and x_{g0} are initial points. Switching is modulated by borders for each subsystem; that is, whenever φ or ψ hits the border specifically defined for one subsystem, switching occurs. Suppose borders for S_1 and S_2 are given by $B_1 = \{x \in R^n : \beta_1(x, t) = 0\}$ and $B_2 = \{x \in R^n : \beta_2(x, t) = 0\}$, respectively. Then, the simplest solution flow can be formulated as

$$\begin{aligned} x_1 &= \varphi(\tau_1, x_0) \\ x_2 &= \psi(\tau_2 - \tau_1, x_1) \\ \beta_1(x_1, \tau_1) &= 0 \\ \beta_2(x_2, \tau_2) &= 0 \end{aligned} \quad (3)$$

where x_0 is the starting point and x_2 is the ending point of the flow, and τ_1 and τ_2 are switching times. Thus, if $x_2 = x_0$, it becomes a periodic solution with the period τ_2 . Moreover, x_1 is the ending point of the first interval as well as the starting point of the second interval. Clearly, switching points must satisfy the border functions $\beta_1 = 0$ and $\beta_2 = 0$. Finally, as (3) contains $2n + 2$ scalar equations with $2n + 2$ scalar unknowns, i.e., $\{x_0, x_1, \tau_1, \tau_2\}$, we can solve the periodic solution using an appropriate numerical method.

The method described earlier does not discriminate the stability status of the periodic solution being found. So, unstable solutions can be found by application of appropriate numerical procedures. To determine the stability of the computed periodic solution, one needs to find the Jacobian of the map $F : R^n \rightarrow R^n$; $x_0 \mapsto x_2$, for the solution flow given in (3), and preferably in terms of $\partial x_2 / \partial x_0$.

From the first two equations of (3), we get

$$\frac{\partial x_1}{\partial x_0} = \frac{\partial \varphi}{\partial t} \frac{\partial \tau_1}{\partial x_0} + \frac{\partial \varphi}{\partial x_0} \quad (4)$$

$$\frac{\partial x_2}{\partial x_0} = \frac{\partial \psi}{\partial t} \frac{\partial \tau_2}{\partial x_0} - \frac{\partial \psi}{\partial t} \frac{\partial \tau_1}{\partial x_0} + \frac{\partial \psi}{\partial x_1} \frac{\partial x_1}{\partial x_0} \quad (5)$$

where φ and ψ denote $\varphi(\tau_1, x_0)$ and $\psi(\tau_2 - \tau_1, x_1)$, respectively. Moreover, from the border functions [i.e., last two equations in (3)], we have

$$\frac{\partial \beta_1}{\partial x_0} = \frac{\partial \beta_1}{\partial x} \frac{\partial x_1}{\partial x_0} + \frac{\partial \beta_1}{\partial t} \frac{\partial \tau_1}{\partial x_0} = 0 \quad (6)$$

$$\frac{\partial \beta_2}{\partial x_0} = \frac{\partial \beta_2}{\partial x} \frac{\partial x_2}{\partial x_0} + \frac{\partial \beta_2}{\partial t} \frac{\partial \tau_2}{\partial x_0} = 0. \quad (7)$$

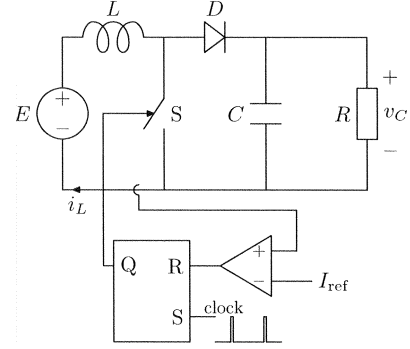


Fig. 1. Current-mode controlled boost converter.

Hence, $\partial \tau_2 / \partial x_0$, $\partial \tau_1 / \partial x_0$ and $\partial x_1 / \partial x_0$ can be obtained easily. Direct substitution yields

$$\frac{\partial x_2}{\partial x_0} = \frac{\left(\frac{\partial \psi}{\partial x_1} \frac{\partial \beta_1}{\partial t} + \frac{\partial \psi}{\partial t} \frac{\partial \beta_1}{\partial x} \right) \frac{\partial \varphi}{\partial x_0} \frac{\partial \beta_2}{\partial t}}{\left(\frac{\partial \beta_2}{\partial t} + \frac{\partial \psi}{\partial t} \frac{\partial \beta_2}{\partial x} \right) \left(\frac{\partial \beta_1}{\partial t} + \frac{\partial \varphi}{\partial t} \frac{\partial \beta_1}{\partial x} \right)}. \quad (8)$$

All terms in the above equation can be calculated by an appropriate numerical method. Thus, by finding the roots of the characteristic equation, we can determine the stability of any periodic solution.

IV. ILLUSTRATION OF MAIN FINDINGS

In much of the previous study, border collision has been shown to exhibit a “jump” in the bifurcation diagram, as a stable operating orbit suddenly gives way to another stable orbit in a discontinuous fashion. Border collision “terminates” a specific solution and the system “jumps” to another attractor. The resulting solution is entirely new and seems to have little relation with the original solution assumed before the onset of border collision. In the following, we will illustrate that the new solution is often generated by a saddle-node bifurcation. In fact, saddle-node bifurcation gives birth to a node and a saddle. While the node can be directly observed, the saddle (or the unstable solution) is invisible and much less considered.

The problem is best illustrated with examples. We will consider the current-mode controlled boost dc–dc converter and the voltage-mode controlled buck dc–dc converters. As the general bifurcation scenarios of both systems are well known [8], they provide very accessible examples on which to explain the subtle connection between the coexisting border collision and saddle-node bifurcation.

Example 1: Current-Mode Controlled Boost Converter: In the current-mode controlled boost converter circuit shown in Fig. 1 [9], [10], the switch is turned on periodically and turned off whenever the current of the inductor reaches a reference value. Thus, the two subsystems are given by

$$S_1 : \dot{x} = \begin{bmatrix} -\frac{1}{RC} & 0 \\ 0 & 0 \end{bmatrix} x + \begin{bmatrix} 0 \\ \frac{1}{L} \end{bmatrix} E \quad (9)$$

$$S_2 : \dot{x} = \begin{bmatrix} -\frac{1}{RC} & \frac{1}{C} \\ -\frac{1}{L} & 0 \end{bmatrix} x + \begin{bmatrix} 0 \\ \frac{1}{L} \end{bmatrix} E. \quad (10)$$

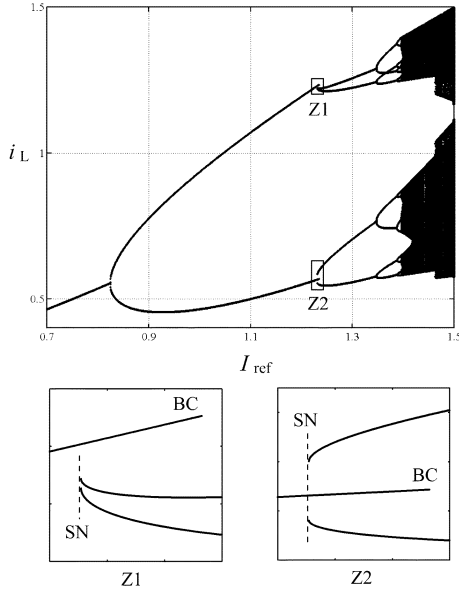


Fig. 2. One-parameter bifurcation diagram of current-mode controlled boost converter, with two blow-up views of regions Z1 and Z2. Parameters are $R = 40 \Omega$, $L = 1.5 \text{ mH}$, $T = 100 \mu\text{s}$, $\tau_C = RC/T = 2$, and $E = 10 \text{ V}$.

When it works in continuous conduction mode, the two borders can be described by

$$B_1 = \{(x, t) \in \mathbb{R}^2 \times \mathbb{R} : \beta_1 = i_L - I_{\text{ref}} = 0\} \quad (11)$$

$$B_2 = \{(x, t) \in \mathbb{R}^2 \times \mathbb{R} : \beta_2 = t - kT = 0\} \quad (12)$$

where $x = [v_C \ i_L]^T$. A typical one-parameter bifurcation diagram is shown in Fig. 2, where the reference current I_{ref} is the bifurcation parameter and the sampled i_L is the variable. Here, as revealed from the blow-up views, as I_{ref} increases, border collision takes place to terminate the period-2 solution, and the system jumps to a period-4 solution. Moreover, if we move backward (decreasing I_{ref}), we see that the period-4 solution ends up at a saddle-node bifurcation, and the solution jumps back to the original period-2 solution.

Although only a stable period-4 solution is observed, an unstable period-4 solution exists. This unstable period-4 solution, being unobservable, has been rarely noticed, let alone discussed. Using the method introduced previously, however, we can track the position of the unstable solutions easily. The results are shown in Fig. 3, where unstable period-4 solutions are traced and shown as dashed curves.

The key message of Fig. 3 is that unstable solutions are also terminated by the same border collision. In other words, the stable period-2 solution and the unstable period-4 solution are terminated by the same border collision. Thus, we see that the border collision is actually being linked to the saddle-node bifurcation by the unstable period-4 solution.

Example 2: Voltage-Mode Controlled Buck Converter: Next, we consider a voltage-mode controlled buck converter [6], as shown in Fig. 4. A feedback signal V_{con} is compared with a ramp voltage signal V_{ramp} to control the switch. Therefore, we can write the two subsystems as

$$S_1 : \dot{x} = \begin{bmatrix} -\frac{1}{RC} & \frac{1}{C} \\ -\frac{1}{L} & 0 \end{bmatrix} x \quad (13)$$

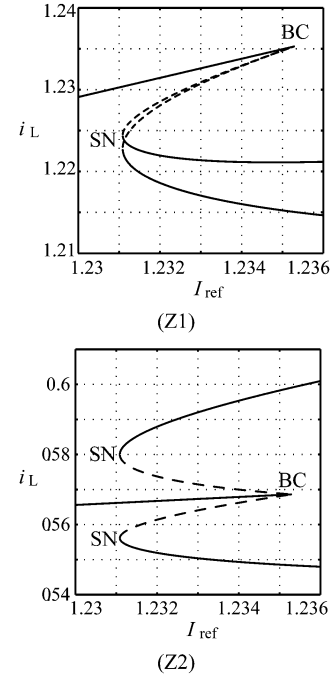


Fig. 3. Blow-up views of the one-parameter bifurcation diagram showing bifurcations of unstable solutions. Parameters are the same as those in Fig. 2.

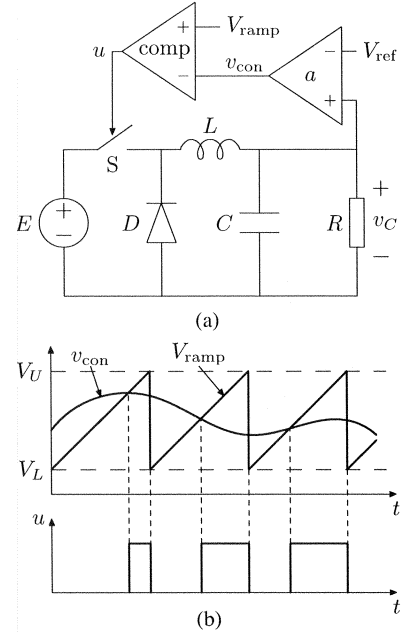


Fig. 4. Voltage-mode controlled buck converter. (a) Circuit schematic. (b) Typical control waveforms.

$$S_2 : \dot{x} = \begin{bmatrix} -\frac{1}{RC} & \frac{1}{C} \\ -\frac{1}{L} & 0 \end{bmatrix} x + \begin{bmatrix} 0 \\ \frac{1}{L} \end{bmatrix} E \quad (14)$$

where $x = [v_C \ i_L]^T$. The border of this system is defined as

$$\begin{aligned} \beta_1(x, t) &= \beta_2(x, t) \\ &= a(v_C - V_{\text{ref}}) - \frac{(V_U - V_L)t}{T} - V_L = 0 \end{aligned} \quad (15)$$

for $t \in [0, T]$, which is a common border for the two subsystems.

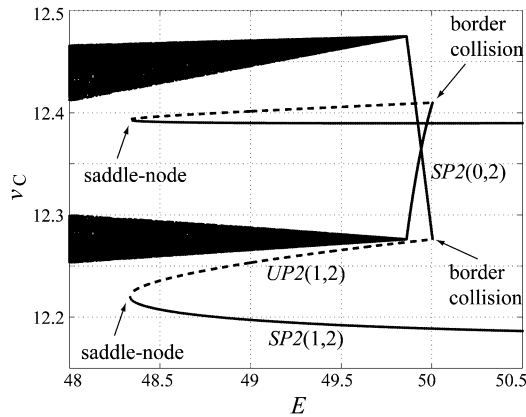


Fig. 5. One-parameter bifurcation diagram from voltage-mode controlled buck converter.

Our previous studies [6] have shown that a period-2 solution can jump to another stable period-2 solution via a border collision, as shown in Fig. 5. Here, we track the unstable period-2 solution generated from saddle-node bifurcation and observe a similar phenomenon. As denoted by dashed curves in Fig. 5, the unstable solution conjoins with the stable solution at the border collision point. Moreover, the paired solutions (stable and unstable) generated by saddle-node bifurcation are having the same switching sequence, in which switching occurs once in the first cycle and twice in the second cycle [denoted symbolically as $SP(1,2)$ and $UP(1,2)$]. Moreover, the stable solution that collides with $UP(1,2)$ has a different switching sequence, in which no switching occurs in the first cycle and two in the second cycle [denoted symbolically as $SP(0,2)$]. When border collision takes place, both stable ($SP(0,2)$) and unstable ($UP(1,2)$) solution flows hit the upper tip of V_{ramp} .

V. DETAILS OF THE BIFURCATION CONNECTION AND INTERACTION

We have already described how stable solutions connected to different bifurcations are tied together by unstable solutions. This is similar to the phenomenon of *hysteresis*, which is often found in systems with resonating states associated with saddle-node bifurcation. At this point, it is instructive to recall the familiar behavior of the Duffing's equation shown simplistically in Fig. 6. Here, curves A , B , and C indicate the resonant amplitude characteristics corresponding to movements of parameters along the horizontal lines A' , B' , and C' . In the case of parameter movement along A' , the solution moves along the solid curves in the arrow direction in Fig. 6(a). When it comes to the point with vertical tangency, a slight change of parameter $p1$ will cause a discontinuous jump of the amplitude to the upper or lower portion of the curve. Between the two bifurcation curves in Fig. 6(b), coexistence of the one unstable and two stable resonant solutions is possible. Moreover, as we increase $p2$, the two bifurcation curves in Fig. 6(b) will move closer to each other. For example, along line B' , the coexistence region is much narrower than that along line A' . Finally, for the case of movement along line C' , i.e., beyond the cusp point P of the bifurcation curves, no bifurcation occurs for the solution and coexistence is no longer observed.

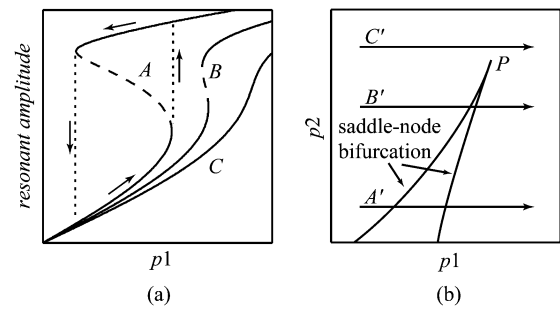


Fig. 6. Illustration of jump and hysteresis phenomena. (a) One-parameter bifurcation diagram; (b) two-parameter bifurcation diagram. Varying parameter $p1$ along lines A , B and C in (b), we get three curves of resonant amplitude characteristics in (a).

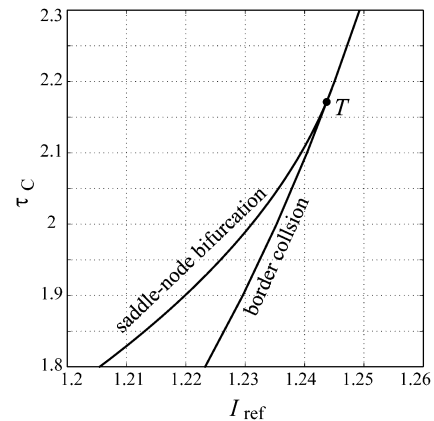


Fig. 7. Bifurcation diagram of boost converter with the same set of parameters as Fig. 2.

Returning to our switched systems, from Figs. 3 and 5, we see that saddle-node bifurcation and border collision are articulated in a similar manner as the aforementioned jump and hysteresis phenomenon.

We now take a detailed look at the bifurcation behavior of the current-mode controlled boost converter around the region where border collision and saddle-node bifurcation occur. Fig. 7 shows the bifurcation diagram in the (I_{ref}, τ_C) plane. Here, we see that the saddle-node bifurcation curve merges tangentially with the border collision curve at point T . Stable period-2 solutions exist on the left-hand side of the border collision curve and stable period-4 solutions exist on the right-hand side of the saddle-node bifurcation curve. Thus, between the two bifurcation curves, coexistence and hysteresis can be observed, as shown in Fig. 3, where $\tau_C = 2$. Similar to the situation illustrated by the Duffing's system (Fig. 6), increasing τ_C above the tangent point T will make saddle-node bifurcation vanish. However, the border collision still remains. If we move parameter I_{ref} along the line $\tau_C = 2.3$, we get a one-parameter bifurcation diagram, as shown in Fig. 8. Comparing with Fig. 3, we see that unstable solutions disappear due to the tangential merger of border collision and saddle-node bifurcation. Finally, the scenes shown in Fig. 8 look deceptively like a period-doubling bifurcation (in some literatures, this situation is called period-adding). Here, it is clear that they are the results of the interaction between saddle-node bifurcation and border collision, corresponding to the choice of parameters above the tangent point T .

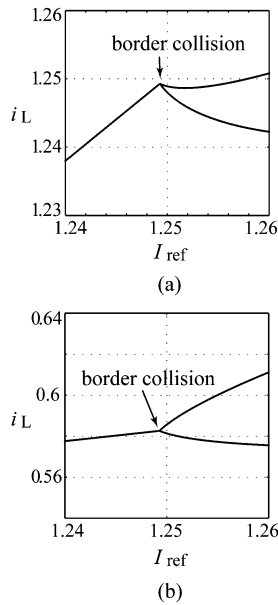


Fig. 8. One-parameter bifurcation diagrams showing no hysteresis jump, with $\tau_C = 2.3$. This corresponds to the case above the tangent point T in Fig. 2.

Similar phenomena can also be observed in the buck converter. As R is decreased, the saddle-node bifurcation will merge tangentially with the border collision (see Fig. 5), and the two period-2 solutions will be connected together (one can refer to Fig. 6(b) in [6]).

The coincidence of Duffing's system and a switched dynamical system is a very useful hint to understand and uncover the relation between border collision and those standard bifurcations. It clearly explains why border collision may manifest itself as a jump (*hard* border collision) or as a continuous turning point (*soft* border collision), depending upon the parameter values being below or above the tangent (merging) point.

VI. CONCLUSION

Being fundamentally different in the underlying bifurcation mechanisms, border collision and saddle-node bifurcation have rarely been considered in a unified way. In this brief, we have discussed the relation between border collision and saddle-node

bifurcation and identified the way in which the two bifurcations are connected. The key finding is that border collision is connected to saddle-node bifurcation via unstable solutions that have been generated by the same saddle-node bifurcation. This explains the jump phenomenon that occurs at border collision. Moreover, as parameters vary, the border collision and the saddle-node bifurcation points merge tangentially. Beyond this merger point, border collision no longer manifests as jumps, but rather as continuous transitions which typically resemble turning points with possible period-multiplying in one-parameter bifurcation diagrams.

Note that the present paper is based on two observed examples, instead of a rigorous theoretical proof. Thus, we cannot cover all the cases, although many observed phenomena can be explained in a likewise manner. Nonetheless, the behavior of unstable solutions, which plays a subtle but important role in governing the overall behavior of nonlinear systems, is an interesting problem for future research.

REFERENCES

- [1] H. Nusse, E. Ott, and J. Yorke, "Border-collision bifurcations: An explanation for observed bifurcation phenomena," *Phys. Rev. E, Stat. Phys. Plasmas Fluids Relat. Interdiscip. Top.*, vol. 49, pp. 1073–1076, 1994.
- [2] G. Yuan, S. Banerjee, E. Ott, and J. A. Yorke, "Border-collision bifurcation in the buck converter," *IEEE Trans. Circuits Syst. I, Fundam. Theory Appl.*, vol. 45, no. 7, pp. 707–716, Jul. 1998.
- [3] S. Banerjee, P. Ranjan, and C. Grebogi, "Bifurcation in two-dimensional piecewise smooth maps—Theory and applications in switching circuits," *IEEE Trans. Circuits Syst. I, Fundam. Theory Appl.*, vol. 47, no. 5, pp. 633–643, May 2000.
- [4] M. di Bernardo, C. J. Budd, and A. R. Champneys, "Grazing and border-collision in piecewise-smooth systems: A unified analytical framework," *Phys. Rev. Lett.*, vol. 86, no. 12, pp. 2553–2556, Mar. 2001.
- [5] C. K. Tse, *Complex Behavior of Switching Power Converters*. Boca Raton, FL: CRC Press, 2003.
- [6] Y. Ma, H. Kawakami, and C. K. Tse, "Analysis of bifurcation in switched dynamical systems with periodically moving borders," *IEEE Trans. Circuit Syst. I, Reg. Papers*, vol. 51, no. 6, pp. 1184–1193, Jun. 2004.
- [7] K. T. Alligood, T. D. Sauer, and J. A. Yorke, *Chaos: An Introduction to Dynamical Systems*. New York: Springer-Verlag, 1996.
- [8] C. K. Tse and M. di Bernardo, "Complex behavior of switching power converters," *Proc. IEEE*, vol. 90, no. 5, pp. 768–781, May 2002.
- [9] J. H. B. Deane, "Chaos in a current-mode controlled boost converter," *IEEE Trans. Circuits Syst. I, Fundam. Theory Appl.*, vol. 39, no. 8, pp. 680–683, Aug. 1992.
- [10] W. C. Y. Chan and C. K. Tse, "Study of bifurcations in current-programmed dc/dc boost converter: From quasi-periodicity to period-doubling," *IEEE Trans. Circuits Syst. I, Fundam. Theory Appl.*, vol. 4, no. 12, pp. 1129–1142, Dec. 1997.